

**NUMERICAL SIMULATIONS OF SHOCK MELTING IN OBLIQUE IMPACTS.** X.-Z. Luo<sup>1</sup>, M.-H. Zhu<sup>1</sup>, M. Ding<sup>1</sup>, L. Manske<sup>2</sup>, R. Luther<sup>2</sup>, and K. Wünnemann<sup>2,3</sup>. <sup>1</sup>State Key Laboratory of Lunar and Planetary Sciences, Macau University of Science and Technology, Macau, China (mhzhu@must.edu.mo); <sup>2</sup>Museum für Naturkunde Berlin, Germany; <sup>3</sup>Freie Universität Berlin, Germany

**Introduction:** Hypervelocity impacts induce strong shock waves that cause a sudden increase of temperature and pressure in the target. A roughly spherical zone adjacent to the surface is melted or vaporized [1, 2]. The volume of the impact-induced melt and vapor zone is critical to investigate the bombardment effects on planets. Numerous studies exist quantifying melt production of vertical impacts [1-6]. However, nearly all impacts on planetary surfaces occur at oblique angles [7, 8], which require full 3D simulations to determine melt production. Because of the high computational costs, systematic studies are lacking. We performed a systematic suite of numerical simulations to quantify melt production for oblique impacts on the Moon. Our ultimate goal is to develop a scaling law (e.g., [9]) relating impact parameters (angle, velocity, and impactor size), with crater dimensions (diameter and volume), and the shockwave-induced melt volume.

**Scaling of Impact Melt for Oblique Impacts:** Dimensional analysis [10] shows that the mass of melt  $M_{melt}$  generated by a given vertical impact scales with the impact velocity,  $U$ :

$$\frac{M_{melt}}{m_p} = k \left( \frac{U^2}{E_M} \right)^{3\mu/2} \quad (1)$$

where  $m_p$  is the mass of the impactor,  $E_M$  is the internal energy of melting, and  $k, \mu$  are the scaling parameters [2, 3, 10, 11].

*Abramov et al.* [9] proposed a melt volume scaling law for oblique impacts based on a numerical study [12]. They assume that when impact angle is the only varied parameter, the melt volume is proportional to the transient crater volume,  $V_{tc}$ , which scales with the impact angle,  $\theta$  [13-15] as:

$$V_{tc} = \frac{\pi \rho_p}{6 \rho_t} C_v (1.61g)^{-\gamma} D_p^{3-\gamma} U^{2\gamma} \sin^{2\gamma}(\theta) \quad (2)$$

where  $\rho_p$  and  $\rho_t$  are the densities of the impactor and target,  $g$  is gravity,  $D_p$  is the impactor diameter, and  $C_v$  and  $\gamma$  are scaling parameters in the  $\pi$ -group scaling relations [16]. According to *Abramov et al.* [9], the melt volume of oblique impacts is given by:

$$\frac{V_{melt}}{V_p} = \frac{\rho_p}{\rho_t} k \left( \frac{U^2}{E_M} \right)^{3\mu/2} \sin^\alpha(\theta) \quad (3)$$

where  $\alpha = 1.3$  taking  $\gamma = 0.66$  for large-scale cratering in rock [13].

Note that these scaling laws do not consider the effect of pre-impact temperature of the target, which directly influences the melt volume [3, 5]. As

temperature increases with depth, larger impacts are more affected by the planet's temperature state. In addition, decompression melting of the uplifted target material in large impacts also generates more melt than the scaling law-predicted value [5].

**Methods:** We use the shock physics code iSALE-3D [13] to quantify the effect of impact angle and impactor size on the melt volume for impacts on the Moon. We carried out a suite of simulations with impactor diameters ranging from 1 to 30 km and impact angles from 90° (vertical impact) to 20° for a typical impact velocity of 15 km s<sup>-1</sup>. We employ the ANEOS of dunite [17, 18] and an elastic-plastic constitutive model [19] to describe the physical and dynamical behavior of impactor and target materials. The material parameters are similar to [20]. We use a thermal profile with a relatively low temperature gradient of 10 K km<sup>-1</sup> in the target [21]. We do not consider the effect of porosity in this work.

Each model is run until the end of the crater modification stage. To determine the transient crater volume, following [5], we track the integrated maximum cavity at all timesteps and sum up the empty cells below the pre-impact surface as the transient crater volume.

To quantify the production of melt, we follow the approach in [5], using the classical peak pressure method [2-4, 10-12, 22], which has been improved to consider the effects of the thermal state of the target and decompression melting. We obtain the peak shock pressure and final pressure of material from the simulation and calculate the isentropic release from the shock state to the final state using the ANEOS code [17]. We quantify all material with final temperature exceeding the dunite solidus as melt. The resulting volume includes the amount of vapor; however, this volume is negligible due to the chosen impact velocity of only 15 km/s.

**Results:** Fig. 1 shows the melt volume normalized by the impactor volume for our simulation results. For impactor diameters of 1 to 30 km, the ratio of  $V_{melt}/V_p$  is roughly constant, indicating that the effect of the assumed temperature gradient is negligible for the given size range. The melt volume increases monotonically with the impact angle. Using  $\mu = 0.56$  as suggested by *Abramov et al.* [9], we fit our normalized melt volumes for impact angles larger than 30° to Eq. 3 and obtain scaling parameters of  $k = 0.26$  and  $\alpha = 1.09$  (magenta curve), which is slightly different from the scaling law by [9] (gray curve) assuming  $E_M = 9 \times 10^6$  J kg<sup>-1</sup> (for

dunite from [2]). Our derived  $k$  is between the values of 0.16 and 0.33 from the numerical studies of *Pierazzo et al.* [2] and *Barr & Citron* [3], respectively. The value of  $k$  varies with the choice of  $\mu$ . Using the theoretical value of energy scaling (2/3) for  $\mu$ , our best fit line yields  $k = 0.16$ .

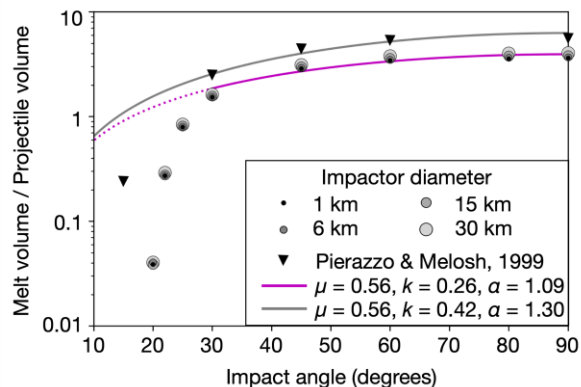


**Fig. 1.** Melt volumes normalized by the impactor volume as a function of impact angle. Circles: the simulation results in this work. Triangles: Simulation results from [22]. Magenta line: Best fit to the scaling law Eq. 3 using our results for  $\theta > 30^\circ$ . Gray line: Scaling law with scaling parameters from [9].

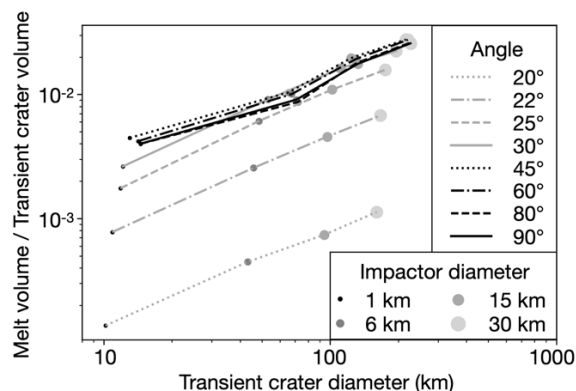


**Fig. 2.** Melt volumes scaled by the transient crater volume as a function of the transient crater diameter for different impact angles and impactor diameters.

Fig. 2 shows our modelled melt volumes scaled by the transient crater volume as a function of the transient crater diameter. For all impact angles,  $V_{melt}/V_{tc}$  increases monotonically with crater diameter. For  $\theta > 30^\circ$ ,  $V_{melt}/V_{tc}$  are roughly the same for different impact angles. For  $\theta < 30^\circ$ ,  $V_{melt}/V_{tc}$  decreases by more than an order of magnitude from  $30^\circ$  to  $20^\circ$ .

**Discussion:** Our results (Fig. 1) show that the melt volume of highly oblique impacts (close to grazing impacts) decreases faster with impact angle than predicted by the scaling law. The ratio of the melt volume-to-transient crater volume also decreases with

impact angle for highly oblique impacts (Fig. 2), which disagrees with the premise of the scaling law in [9] (Eq. 3).

We note that the melt volume for low-angle impacts could be underestimated as we do not consider heating due to plastic work [6, 23], which may not be negligible for highly oblique impacts.

The spatial resolution of the model could significantly affect the melt volume as noted by [2, 3, 24]. For all models, we employ a spatial resolution of 15 cells per projectile radius. Our resolution tests show that we may underestimate the melt volume by 20% with such a resolution.

During the impact excavation process, a fraction of melt is ejected out of the crater cavity and is deposited around the crater. *Luo et al.* [25] shows that the ejecta patterns from oblique impacts are affected by the impact angle and impactor diameter. The result of this work will be combined with ejecta deposition calculation to investigate the melt deposit pattern for craters on the Moon, similar to *Liu et al.* [26].

**Conclusions:** We simulate crater formation and impact melting with different impact angles and impactor sizes to derive a scaling law for the melt volume in oblique impacts. Our results show that for impactor diameters up to 30 km, the impact scale does not affect the melt volume-to-impactor volume ratio for a cold thermal profile of the Moon. Considering shock melting only, melt volumes of low angle impacts deviate from a scaling relationship [9] that assumes constant melt volume-to-transient crater volume ratio for all impact angles.

**Acknowledgments:** This work is supported by the Science and Technology Development Fund, Macau (0020/2021/A1; 0064/2022/A2), NSFC 12173106 and Germany Science Foundation (DFG), TRR170, C4. We thank the iSALE developers.

**References:** [1] Croft (1982) *GSA Special Papers*, 190, 143-152 [2] Pierazzo et al. (1997) *Icarus*, 127, 408-423 [3] Barr & Citron (2011) *Icarus*, 211, 913-916 [4] Wünnemann et al. (2008) *EPSL*, 269, 530-539 [5] Manske et al. (2021) *Icarus*, 357, 1141-128 [6] Manske et al. (2022) *JGR*, 127, e2022JE007426 [7] Gilbert (1893) *Bull. Philos. Soc. Wash.*, XII, 241-292 [8] Shoemaker (1962) *Physics and Astronomy of the Moon*, 283-359 [9] Abramov et al. (2012) *Icarus*, 218, 906-916 [10] Bjorkman & Holsapple (1987) *Int. J. Impact Eng.*, 5, 155-163 [11] Ahrens & O'Keefe (1977) *Impact and Explosion Cratering*, 639-656 [12] Pierazzo & Melosh (2000) *Icarus*, 145, 252-261 [13] Elbeshhausen et al. (2009) *Icarus*, 204, 716-731 [14] Davison et al. (2011) *M&PS*, 46, 1510-1524 [15] Gault & Wedekind (1978) *Proc. LPSC*, 9, 3843-3875 [16] Schmidt & Housen (1987) *Int. J. Impact Eng.*, 5, 543-560 [17] Thompson (1990) *Sandia Nat'l. Lab* [18] Benz et al. (1989) *Icarus*, 81, 113-131 [19] Collin et al. (2004) *M&PS*, 39, 217-231 [20] Potter et al. (2013) *JGR*, 118, 963-979 [21] Spohn et al. (2001) *Icarus*, 149, 54-65 [22] Pierazzo & Melosh (1999) *EPSL*, 165, 163-176 [23] Kurosawa & Genda (2018) *GRL*, 45, 620-626 [24] Davison et al. (2014) *M&PS*, 49, 2252-2265 [25] Luo et al. (2022) *JGR*, 127, e2022JE007333 [26] Liu et al. (2022) *JGR*, 127, e2022JE007264